

BLINDNESS EFFECTS IN GROUND PLANE-BACKED TEM HORN ARRAYS

Daniel T. McGrath
US Air Force Research Laboratory
Kirtland AFB, NM

INTRODUCTION

Arrays of TEM (transverse electromagnetic) horn antennas are possible candidates for ultrawideband (UWB) applications. Those applications require focused radiation or reception of transient waveforms without dispersion. Previous work showed that the useful bandwidth of TEM horn arrays extended from the grating lobe limit down to that frequency at which the entire antenna is one half wavelength across [1]. However, due to the fact that they are open to free space in both directions, there is considerable back lobe energy. When a ground plane is added to prevent the back lobe radiation, a scan blindness appears due the presence of a trapped wave mode between the horns and the ground plane. This paper summarizes numerical experiments that characterize this blindness phenomenon.

TEM HORN ARRAY DESCRIPTION AND ANALYSIS APPROACH

Fig. 1a shows the basic geometry of a TEM horn array. The sources or loads are located at the apices, and the horns are joined to one another at their mouths. Fig. 1b shows a unit cell for one of the particular cases, whose aperture has a 2:1 aspect ratio ($d_x = 2 d_y = \lambda_0$). Fig. 1c is a variant whose profile in the y - z plane is an exponential flare, similar to that used for notch antennas [2]. Fig. 1d is an expanded view of the feed region in both Figs. 1b and 1c. The ground plane is located at the geometric horn apex, which is $.025 \cdot d$ from the feed point. In the results presented below, the feed-to-ground plane distance scales with the array height, d .

The analysis of the transmitting and receiving properties of these arrays used a frequency-domain hybrid finite element method that incorporates periodic boundary conditions [3], which accounts for array mutual coupling effects. The infinite array assumption limits the analysis to a single unit cell. This will provide accurate results for gain and input impedance of large, finite arrays. However, a finite array will not radiate efficiently at frequencies below that at which it is one half wavelength across, so infinite array calculations are not meaningful below that frequency. All results are shown in frequency normalized to f_0 , the frequency at which the unit cell width in x is one wavelength.

The field inside the unit cell is expanded in linear, edge-based vector elements. The finite element region is terminated at the $z=0$ plane (the horn mouth) with a periodic radiation condition. The $z=d$ plane is the ground plane. Periodicity conditions are also imposed to connect opposing sides in x and y . This formulation leads to a system of equations that must be solved independently for each scan angle and frequency. In the receiving case, the excitation is a plane wave impinging on the horn aperture from the $-z$ direction, and the response is the current through a load at the feed point.

INPUT IMPEDANCE

The high frequency limit of input impedance for a TEM horn array is simply that of an isolated horn, which can be determined analytically using conformal and stereographic projections [4]. For the 2:1 aspect ratio horn, it is approximately 105 Ω . With a ground plane, the low frequency limit is 0 Ω .

Fig. 2 shows the real part of Z_{in} for the linear flare horn, for three different values of d , at broadside scan. Over the frequency range where Z_{in} is most constant it is close to, but somewhat higher than the high frequency limit prediction. When $d = \lambda_0$, $\text{Re}\{Z_{in}\}$ goes through 0 Ω near $f = .65 f_0$. This is the blindness, which is observed to move up in frequency as the array height, d , decreases. With $d = .5\lambda_0$, it is just below the grating lobe limiting frequency f_0 . Results are similar for the exponential flare horn, with nearly the same blindness frequencies. However, the input impedance is substantially lower than that of the linear flare horn. Consequently, the results shown below for received power use 105 Ω and 75 Ω for the load impedances for the linear and exponential horns, respectively.

ARRAY FREQUENCY RESPONSE WITH E-PLANE SCANNING

Fig. 3 shows the ratio of received to incident power for both the linear flare and exponential flare horns, at three different scan angles in the E (y - z) plane. The locations of the scan blindness in angle and frequency are nearly the same for both element designs, which indicates that the horn shape has only a minor effect. The scan blindness displays the unusual property of moving up in frequency with increasing scan angle from broadside. Schaubert [5] showed that a similar phenomenon, observed for flared notch arrays was due to a guided wave mode. In this case, the guided wave mode must be similar to a TM parallel-plate mode between the ground plane and the corrugated surface formed by the horn plates.

CONCLUSIONS

In the course of developing TEM horn arrays for ultrawideband applications, it has been found that a ground plane behind the horns not only prevents low frequency radiation, as expected, but also introduces a scan blindness at frequencies and angles below the grating lobe limits. These blindnesses: 1) move outward in angle with frequency; 2) are fairly insensitive to the horn flare shape; and 3) are most sensitive to the array depth. Due to these features it is postulated that the blindness is caused by a waveguide mode propagating along the array face between the horn plates and the ground plane. This observation will help in predicting the conditions allowing the blindness and possibly lead to methods to prevent its occurrence.

ACKNOWLEDGEMENTS

The success of this work depended largely on computer support from Aeronautical Systems Center (ASC MSRC), Maui High Performance Computing Center, and Waterways Experiment Station (CEWES MSRC). It was funded in part by the Air Force Office of Scientific Research.

REFERENCES

1. McGrath, D.T. and C.E. Baum, "Numerical Analysis of Planar Bicone and TEM Horn Array Antennas," *Digest, 1997 IEEE AP-S Symposium*, Montreal, Canada, Jul. 1997, pp. 1058-1061.
2. Choung, Y.H. and C.C. Chen, "44 GHz Slotline Phased Array Antenna," *Digest, 1989 IEEE AP-S Symposium*, pp. 1730-1733.
3. McGrath, D.T. and V.P. Pyati, "Phased Array Antenna Analysis with the Hybrid Finite Element Method," *IEEE Trans. Antennas Propagat.*, AP-42, Dec. 1994, pp. 1625-1630.
4. Yang, F.C. and K.S.H. Lee, "Impedance of a Two-Conical Plate Transmission Line," *Sensor and Simulation Note #221*, AF Research Laboratory, Kirtland AFB, NM, Nov. 1976.
5. Schaubert, D.H., "A Class of E-Plane Scan Blindnesses in Single-Polarized Arrays of Tapered Slot Antennas with a Ground Plane," *IEEE Trans. Antennas Propagat.*, AP-44, Jul. 1996, pp. 954-959.

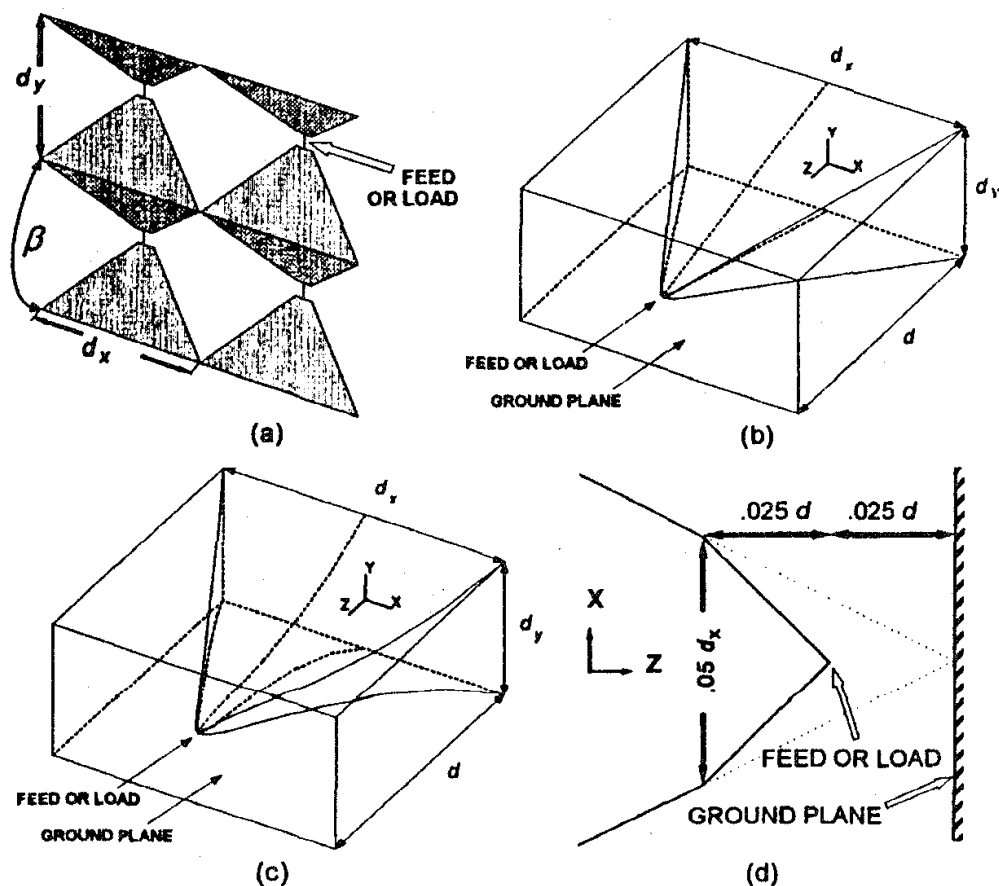


Figure 1. Geometry: (a) Generic TEM Horn Array; (b) Unit Cell Model with Linear-Flare Horn; (c) Unit Cell Model with Exponential-Flare Horn; and (d) Feed Region Detail

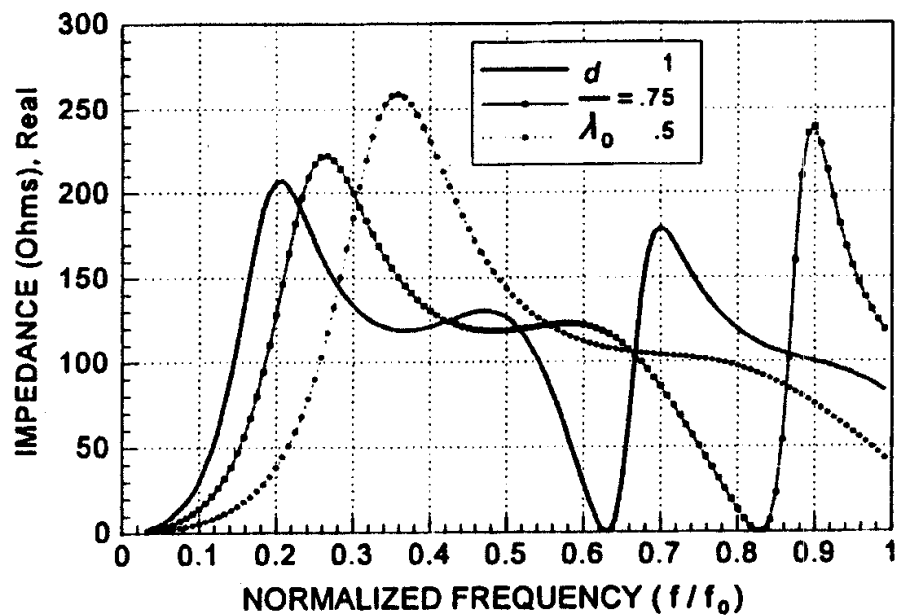


Figure 2. Real Part of Input Impedance vs. Frequency for Linear-Flare TEM Horn Array with three different depths, $d_x = \lambda_0$, $d_y = d_x/2$

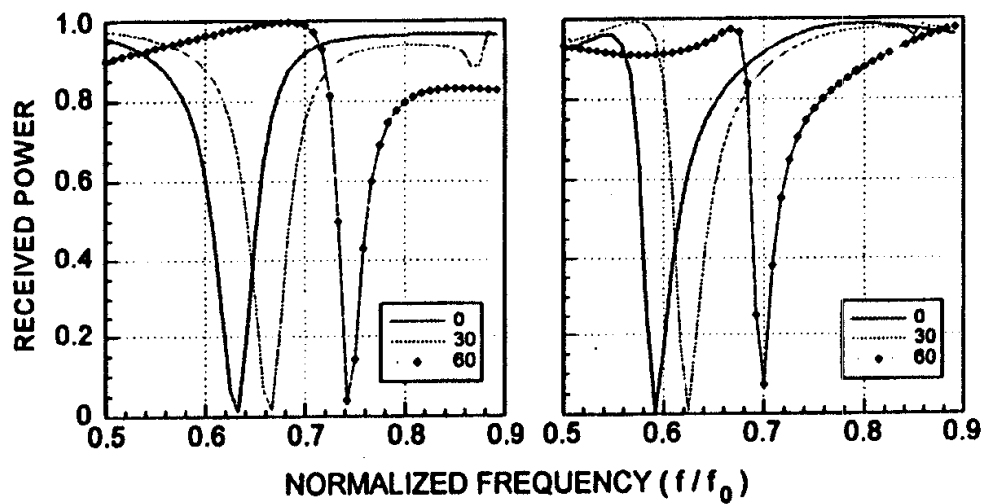


Figure 3. Received Power vs. Frequency at 0°, 30° and 60° Scan in the E Plane: Left, Linear-Flare Horn; and Right, Exponential-Flare Horn